Field programmable gate arrays implementation of a Kalman filter based state of charge observer of a lithium ion battery pack

Khadija El Kadri Benkara, Amalie Alchami, Achraf Nasser Eddine, Ghada Bakaraki, Christophe Forgez

Field Programmable Gate Arrays Implementation of a Kalman Filter Based State of Charge Observer of a Lithium Ion Battery Pack

Khadija El Kadri Benkara, Amalie Alchami, Achraf Nasser Eddine, Ghada Bakaraki, Christophe Forgez.

Université de technologie de Compiègne, Roberval (Mechanics, energy and electricity), Centre de recherche Royallieu - CS 60319 - 60203 Compiègne Cedex – France.

Abstract

This paper presents a study on the state of charge observation of lithium-Ion batteries for energy management in embedded applications. The knowledge of the state of charge is fundamental for the safety and optimal usage of these batteries. The study focuses on the development and implementation of a Kalman filter-based observer algorithm on a Spartan 6 FPGA that can accurately estimate the state of charge of a battery, even if it is initialized differently from its actual state. In this paper we have focused on the opportunities of FPGA for fast calculation which allow to use the FPGA as a slave component in a BMS and allow to observe the SOC a great deal of cells with a low cost. The implementation of this observer on a low-cost FPGA can lead to cost reduction for battery management systems in various applications, such as electric cars and any other systems requiring the observation of the state of charge of a battery pack. The observer model was validated through simulations and real-time testing. This study presents a promising approach to accurately estimate the state of charge of Lithium-Ion batteries for efficient energy management in various applications.

Keywords: Energy management; Lithium-Ion batteries; Battery Management System (BMS), State Of Charge (SOC Estimation), Extended Kalman Filter (EKF) algorithms, Field Programmable Gate Arrays (FPGA Implementation), Real-time Applications.

1. Introduction

Energy management is a crucial aspect of embedded applications, especially in battery-powered devices, as it affects the battery life and the overall performance of the system [1–3]. Lithium-Ion batteries are widely used in various applications due to their high energy density, low self-discharge rate, and long cycle life [4]. To ensure the safety and efficiency of the battery-powered system, the state of charge (SOC) must be accurately estimated. Inaccurate SOC estimation can lead to overcharging, undercharging, and premature battery failure. Accurate estimation of the SOC of Lithium-Ion batteries is a challenging task due to their non-linear and time-varying characteristics [5, 6]. Therefore, several SOC estimation methods have been proposed, including model-based and data-driven approaches [7, 8].

Battery management systems (BMSs) are an essential component of a battery pack, as they monitor the state of the battery and control its charging and discharging processes [9]. Accurate state-of-charge (SOC) estimation is a crucial function of BMSs, as it provides information on the amount of energy remaining in the battery and enables optimal battery usage [10]. Moreover, reliable SOC estimation is necessary to prevent battery overcharging and undercharging, which can significantly reduce battery life and safety [11]. In order to accurately estimate the SOC, the estimation algorithm has to meet the following requirements: high precision to ensure coherent energy management, robustness against some inaccuracies due to the use of low-end sensors in BMS, robustness against the misestimation of the batteries' parameters which highly depend on both temperature and battery degradation and low computational power requirements that allow the use of microcontrollers in the estimation. To achieve accurate SOC estimation, various modeling and estimation techniques have been developed, including electrochemical, equivalent circuit, and data-driven approaches [12–15]. The electrochemical model is widely used due to its accuracy and ability to estimate the internal states of the battery[16]. However, the electrochemical model is computationally expensive and requires a high level of expertise to implement. On the other hand, observer-based methods are relatively simple to implement and provide good estimation accuracy.

Morever, SOC estimation methods can be divided into 2 groups: open loop and closed loop estimation. On the one hand, the open loop group includes: the coulomb counting method that is widely used in SOC estimation. It's simple and easy to be implemented but needs a prior knowledge of the initial SOC. It also has slower dynamic and poor reliability due to the integration. In addition, the open circuit voltage (OCV) method can also be used since it's of high accuracy but needs a long time for the battery to rest. On the other hand, the group of the closed loop methods mainly includes the Model Predictive Control (MPC) which are one of the most effective techniques for cell-level control of the battery packs since it takes into consideration constraints and refines the safety margins allowing the battery to be fully used [17]. We can find a lot of SOC estimation methods based on MPC such as: the Extended Kalman Filter (EKF), the Dual Extended Kalman Filter (DEKF), the Adaptive Extended Kalman Filter (AEKF), the Adaptive Mix Algorithm (AMA), the state observers, the Generalized Extended State Observer (GESO), fuzzy logic methods and neural networks, etc.. . . [18, 19].

Besides, other estimation techniques can be found as well in the literature: In [20], an application of the H infinity filter with the Ni-mH batteries is proposed along with the corresponding results. This method is based on minimizing the H infinity norm of the estimation error. In [21–23], a novel method AMA (Adaptive Mix Algorithm) is introduced, where a state observer is being implemented based on the difference between the output voltage and the battery's measured voltage. Moreover, the authors in [24] presented a new method called Generalized Extended State Observer (GESO). Several other methods can be added to the previously cited techniques such as: the Sliding Mode Observer (SMO) whose idea is explained in [25] and [26]. In order to get out of the box, techniques other than filters are being used in the research domain. For example, a technique based on both neural networks and fuzzy logic can be found in [14, 15, 27, 28]. A comparison between EKF, SMO, H infinity and Luenberger Observer is conducted in [29]. Another estimation approach is used in [30] and [31] which is based on Particle Filter (PF). Additionally, another comparison between PF and EKF is established in [32]. Other Variants of the Kalman Filter can also be deployed to estimate the SOC such as: the Unscented Kalman Filter (UKF) and the Sigma Point Kalman Filter (SPKF) [33–36].

Several methods have been proposed for online estimation of SOC, with state observers, especially the Extended Kalman Filter (EKF), being a popular choice due to their robustness [37–39]. In battery management, the EKF recursive algorithm can be used to estimate the SOC by incorporating the battery model and the measurement data [40]. The cost of implementing sophisticated SOC estimation algorithms using microcontrollers can be high, particularly for systems with hundreds of cells, and may not always be adequate. This BMS cost, including supervision and balancing, may reach up to 30% of the price of the battery pack. Therefore, this paper presents the interest of using Field Programmable Gate Arrays (FPGA) to perform fast calculations of SOC estimation algorithms for EV batteries made up of multiple cells connected in series [17, 18, 41, 42]. FPGA chips can be used not only with batteries, but they proved high effectiveness in the industrial domain [42, 43].

In this paper, we present a study on the state of charge (SOC) observation of Lithium-Ion batteries using an observer based on the Extended Kalman filter algorithm. The main goal is to implement this observer on a Spartan 6 FPGA, which is a low-cost and efficient solution for embedded systems. The proposed observer is capable of correcting the estimated SOC in case it is initialized differently from the actual SOC of the battery. The fast observation time makes it possible to observe multiple batteries simultaneously using the same FPGA, reducing the cost of BMS in electric car systems or any other system requiring the observation of the SOC of a battery pack [44, 45].

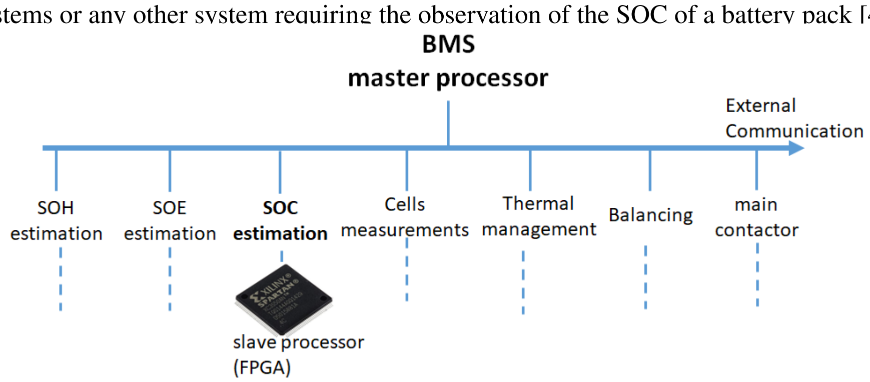

Figure 1: Architecture and functions of a BMS.

The rest of the paper is organized as follows. Section II provides a brief overview of the lithium-Ion battery model used in this study and the observer design based on the Kalman filter algorithm. Section III presents the implementation of the observer on a Spartan 6 FPGA. Section IV provides the simulation With Xilinx environment. Section V describes the experimental results of the proposed observer. Finally, Section VI concludes the paper and discusses future work.

2. State of charge observer

2.1. Battery model

Various approaches have been developed to accurately represent the dynamic behavior of an electrochemical cell. One of these methods involves electrochemical models that use the solution of partial differential equations that describe the chemical reactions taking place within the cell. These models are useful for predicting cell performance and understanding aging mechanisms. However, such an approach requires knowledge of the initial and boundary conditions of the cell, which is not always available. Moreover, the computational complexity of this approach makes it unsuitable for real-time applications. In order to overcome this problem, simplified models based on electric equivalent circuits (EECs) have been developed [46, 47]. EECs provide an alternative solution for modeling polarization due to the phenomena taking place within the battery during its use. EECs are suitable for non-electrochemists and are fairly simple to deploy in real-time applications. However, electrochemical phenomena must be considered at the cell level to simplify the identification of such a model.

Figure 2 depicts the electric equivalent circuit used to model the electrochemical dynamics of each cell within our battery. The circuit includes a voltage source OCV (open-circuit voltage) that refers to the equilibrium potential of the cell and is dependent on the state of charge. Additionally, a resistance R_Ω represents high-frequency phenomena such as electrolyte and connection resistances, as well as the resistance of charge transfer phenomena. Finally, a parallel circuit R_1C_1 symbolizes low-frequency phenomena (diffusion phenomenon).

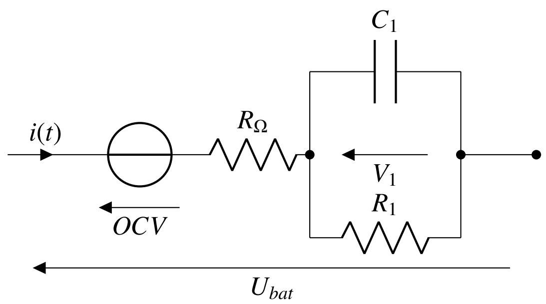

Figure 2: Battery model used in the observer

To simplify the real-time calculations, we propose modeling the diffusion phenomenon with a single *RC* circuit. This first-order representation is sufficient for simulating continuous charge or discharge. We assume a sampling period of $Te = 0.1$ seconds to ensure computational efficiency by the Battery Management System (BMS). In comparison to the sampling period, the dynamic of the charge transfer phenomenon, which occurs at approximately 10 *ms*, is neglected. The cell model's state equation, extended to the state of charge (SOC), is expressed in equation 1:

$$\begin{cases} V_{1_{k+1}} &= \left(1 - \dfrac{Te}{R_1C_1}\right).V_{1_k} + \dfrac{Te}{C1}.i_k \\ SOC_{k+1} &= SOC_k + \left(\dfrac{Te.100}{Qnom}\right).i_k \\ U_{bat_k} &= OCV(SOC_k) + R_\Omega.i_k + V_{1_k} \end{cases} \tag{1}$$

where Q_{nom} is the nominal capacity, V_1 is the voltage across the circuit R_1C_1, SOC is the state of charge, and U_{bat} the terminal battery voltage.

The discrete state battery model extended to the SOC becomes:

$$\begin{aligned} x_{k+1} &= f(x_k, u_k) \\ y_k &= g(x_k, u_k) \end{aligned} \tag{2}$$

where $x_k = [V_{1_k} \quad SOC_k]^T$ and $u_k = [i_k]$.

2.2. *Kalman filter based State of charge observer*

Estimating the State of Charge (SOC) of a battery is a challenging task as it cannot be directly measured. To address this issue, the Extended Kalman Filter (EKF) is widely used in the literature. The EKF requires an accurate mathematical model of the battery and is capable of estimating SOC within a certain range of noise [48].

The EKF consists in initializing and predicting the state variables at a specific sample time Te. The state equation of the cell model, which includes the SOC, is used for the prediction process (equation 1). The performance of the observer depends on the confidence in both the measurements and the model. Therefore, to account for uncertainties in the theoretical model, we consider an uncertainty w_k for the model and an uncertainty v_k for the voltage measurement (Equation 3).

$$\begin{aligned} x_{k+1} &= f(x_k, u_k) + w_k \\ y_k &= g(x_k, u_k) + v_k \end{aligned} \tag{3}$$

In this study, we consider model and measurement uncertainties as white, Gaussian, and centered noises, as commonly assumed in the literature [37, 49]. To incorporate these uncertainties in the state and measurement noise covariance matrices Q and R, respectively, we define $Q = E\{w_k w_k^T\}$ and $R = E\{v_k v_k^T\}$.

However, the battery model extended to the SOC is nonlinear due to the SOC dependency of the open voltage circuit extension. To utilize the Kalman algorithm, the nonlinear battery model extended to the SOC must be linearized at each sample time through the computation of Jacobian matrices, as shown in Equation 4. This linearization step is necessary to enable the use of the Kalman algorithm, which is established on a linear state space model.

$$F_k = \frac{\partial f(x_k, u_k)}{\partial x} \quad G_k = \frac{\partial g(x_k, u_k)}{\partial x} \tag{4}$$

With $G_k$is the state matrice with the term $\frac{\partial OCV}{\partial SOC}$ which is a lookup table in function of SOC.

After linearizing the discrete state space model, a Kalman gain is calculated in relation to the prediction of covariance matrices.

$$K_{k+1} = P_{x,k+1||k} G_{k+1}^T P_{y,k+1||k}^{-1} \tag{5}$$

Then, the covariance matrices are updated

$$\begin{aligned} P_{x,k+1||k} &= F_k P_{x,k||k} F_k^T + Q \\ P_{y,k+1||k} &= G_k P_{x,k+1||k} G_k^T + R \\ P_{x,k+1||k+1} &= P_{x,k+1||k} - K_{k+1} P_{y,k+1||k} K_{k+1}^T \end{aligned} \tag{6}$$

In the final step, the predicted state vector is corrected using the optimal gain K.

$$\hat{x}_{k+1||k+1} = \hat{x}_{k+1||k} + K_{k+1}(y_{k+1} - \hat{y}_{k+1||k}) \tag{7}$$

The parameters of the Extended Kalman Filter are summarized in the Table 1.

	Input variables for each cell	Output and stored variables
Cell voltage	U_{bat_k}	
Cell state of charge	SOC_k	SOC_{k+1}
Current	i_k	
Covariance matrices	$P_{x,k\|\|k}$ $P_{x,k+1\|\|k}$	$P_{x,k+1\|\|k+1}$
Covariance matrices	$P_{y,k\|\|k}$	$P_{y,k+1\|\|k}$
	Stored constants for all cells	
High frequency resistance	R_Ω	
Diffusion resistance	R_1	
Diffusion capacity	C_1	
Nominal capacity	Q_{nom}	
Sampling period	T_e	
Open circuit voltage lookup table	$OCV(SOC_k)$	
Derivative of open circuit voltage in relation to SOC lookup table	$\frac{\partial OCV}{\partial SOC}$	
State covariance matrice	Q	
Measurement noise covariance matrice	R	

Table 1: Parameters of the Kalman filter

3. FPGA implementation

3.1. FPGA-Based Architecture Design

FPGAs consist of two types of resources: processing resources, such as memories, logic, and registers, which are grouped in logic blocks of different types, and programmable interconnection resources that link the logic blocks together. To program a reconfigurable circuit, one must specify the functionality of each logic block and organize the interconnection network to perform the requested function [50].

For this study, we are interested in programmable circuit architectures of the matrix type, in which logic blocks are organized in a regular rectangular structure, with each block connected to the routing network by Programmable Interconnection Points. The routing network is made up of horizontal and vertical channels that occupy the space between the logic blocks.

FPGAs are made up of pre-designed elementary cells and interconnections that are entirely programmable by the end user, allowing for the construction of specific hardware architectures that meet the requirements of the final targeted application [51].

FPGAs have demonstrated their efficacy in the industrial domain, providing high throughput and low latency processing through parallelism and optimized data paths. The flexibility of user-defined circuits enables the association of different data types and precisions, enhancing performance and reducing costs. Additionally, FPGAs are scalable for design improvement and system expansion [28, 52].

The use of FPGAs allows for the configuration of parallelism calculus to execute an algorithm, thereby reducing the execution time of the algorithm. However, programming an FPGA requires the optimization of the physical characteristics that are crucial for the implementation of the algorithm. This optimization is based on two tasks: optimizing the time/area performances required to implement the algorithm and selecting the appropriate number of bits for each data format (variables and coefficients) while maintaining the essential accuracy of the observer.

3.2. Equipments and software

For this study, the aim is to implement the Extended Kalman filter EKF that estimates the state of charge of the pack on a real-time system. To achieve this goal, the MicroAutoBox II (MABXII) 1401/1511/1512 from dSPACE is used, a robust and reliable hardware platform widely used for prototyping and testing in the automotive industry. The

Xilinx Spartan-6 FPGA (XC6SLX150) embedded in the MicroAutoBox II is employed for its high performance and low power consumption

Table 2 summarizes some of the key specifications of this FPGA, which make it suitable for our application.

Process technology	45 nm
Number of Logic Cells (LCs)	147443
Configurable Logic Blocks (CLBs)	
Slices	23038
Flip-Flops	184304
Max Distributed RAM (Kb)	1355
DSP48A1 Slices	180
Max user I/O	576
Memory	4824 Kb
Clock	80 MHz

Table 2: Main specifications of the FPGA

The SOC observer has been implemented on the FPGA of a dSPACE MicroAutoBox II. Moreover, It has undergone testing for estimating the SOC of individual Li-Ion cells within a battery pack consisting of 5 cells connected in series, as depicted in Figure 3. This battery pack serves as a prototype to substantiate the efficacy of the SOC observer method.

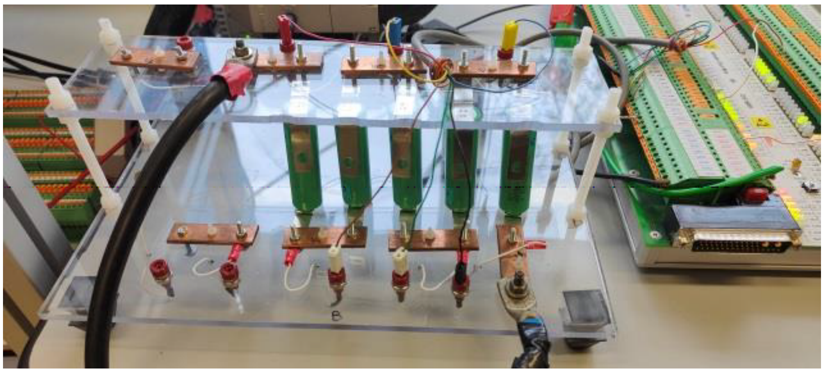

Figure 3: Battery pack made of 5 cells in series.

In our study, we have chosen to use the Samsung 25R 18650 Li-Ion cells, which are a blend of NCA (Nickel Cobalt Aluminum) and NMC (Nickel Manganese Cobalt) chemistries at the positive electrode and with graphite as the negative electrode. Each cell has a nominal capacity of Q_{nom} = 2.5 Ah. The battery pack is designed to operate at a total nominal voltage of 18 V, with each individual cell having a nominal voltage of 3.6 V, and an overall capacity of 2.5 Ah. In previous research, the parameters of the battery model were identified as a function of temperature, SOC, and current using the Galvanostatic Intermittent Titration Technique (GITT) [53, 54]. Figure 4 illustrates the identified impedance parameters at 25 °C.

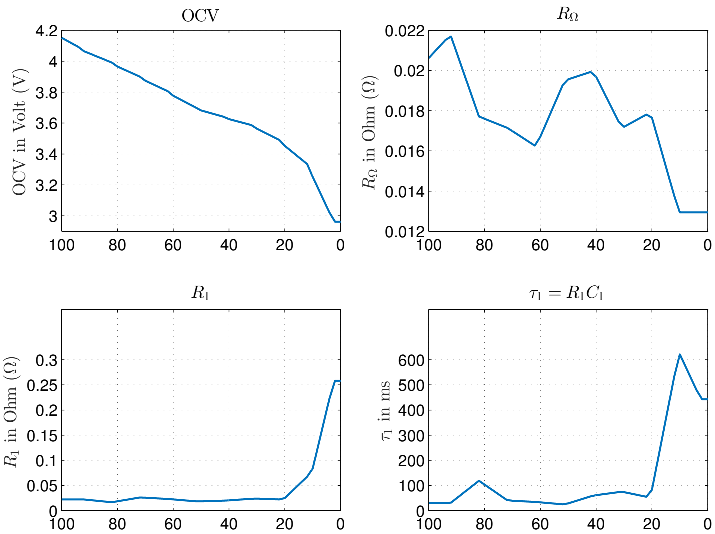

Figure 4: Graphic describing the evolution of the battery parameters in function of the State Of Charge at 25 °C

For the implementation, the battery's temperature was assumed at 25 °C and that its parameters are constant with temperature, SOC, and current. The EKF algorithm was developed using Simulink blocks for FPGA. Figure 5 shows a part of the EKF algorithm written with special Simulink blocks for FPGA which are recognizable by Xilinx's symbol. The design was optimized for performance and resource utilization by utilizing pipelining, time-division multiplexing/folding, and customized precision.

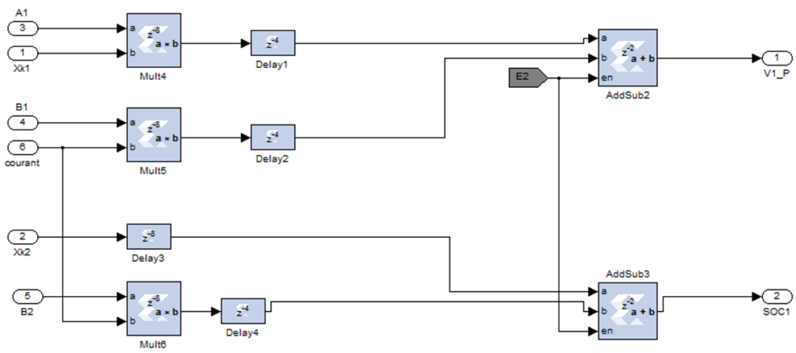

Figure 5: Part of EKF algorithm written with special Simulink blocks for Xilinx FPGA.

3.3. *Time Division Multiplexing Technique*

The battery pack used in this study comprises 5 Li-Ion cells arranged in series. To estimate the state of charge of each cell, two primary approaches are available. The first approach involves developing a design that contains five battery models. However, this method is unsuitable for real-time implementation due to the significant resource demands, necessitating the use of a resource-rich, albeit more expensive FPGA.

The second approach is based on time-division multiplexing, as illustrated in Figure 6. At each sample time $Te' = 0.02s$, the battery pack's current $i(k)$ and cell voltages $Vcell_N(k)$ are digitized using the MicroAutoBox DSP board's analog-digital converter (ADC). Subsequently, a state machine sequentially addresses the data ($I(k)$, $Vcell_N(k)$) to the FPGA, which executes the EKF algorithm. At the end of the EKF algorithm, the estimated and corrected $SOC(k)$, as well as other variables such as error covariance matrices ($P_{x,k+1\|k}P_{y,k+1\|k}$) and diffusion voltage V_{1_k} (denoted V_{diff_k} in Figure 6) required for the next sampling period, are sent to the DSP.

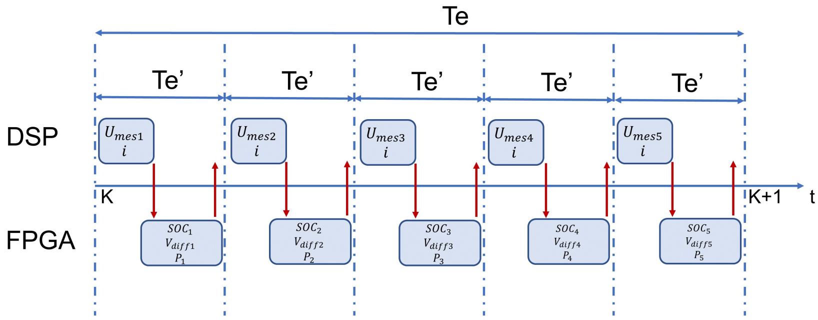

Figure 6: Timing diagram.

In the forthcoming section,the focus will be on the validation of the observer through simulation. This step is crucial in ensuring the accuracy and effectiveness of the observer prior to its deployment on the FPGA.

4. Validation of the observer with Xilinx

In this section, we describe the validation process of the algorithm using the system generator library specifically designed for FPGA programming. This library allows for the FPGA to be programmed with Simulink blocks that can process data in either floating-point mode or fixed-point mode. The results obtained depend on the representation mode used, with greater accuracy requiring more resources in the FPGA. To strike a balance between result precision and resource utilization, we have chosen the signed representation in fixed-point mode, specifically the $Fix32\_16$ format, with 15 bits for the integer part, 16 bits for the decimal part, and one bit for the sign. The main advantage of using this Xilinx library is the ease of implementation on FPGA without requiring VHDL programming, which can be difficult.

In this study, the performance of the EKF-based observer was evaluated using a current profile corresponding to a battery discharge with a current of 1C (2.5 A). The real SOC was initialized to 100%, while the initial estimated value of the state of charge, SOC_0, was set to 0%. It should be noted that SOC_0 is a tunable parameter that allows for a wide range of initialization of the estimated SOC. The SOC reference was obtained through a coulomb meter initialized with the correct initial SOC and the nominal capacity.

To validate our designed estimator, we subjected it to a current profile corresponding to a battery discharge with a current step of 1C (2.5 A).

The obtained results, as shown in Figure 7, indicate that despite being initialized to a value different from the real SOC initial value, the estimated SOC converges towards the real state of charge of the cell. This suggests that the EKF-based observer is capable of correcting a bad estimation of the SOC and enabling the estimated SOC to converge to the real SOC. However, the fixedpoint representation used in the implementation limits the number of bits used, leading to errors in the estimation. In addition, errors may accumulate during the current integration when predicting the state variables, resulting in significant margins of error between the estimated and real variables. Nonetheless, as long as the absolute error is less than 5%, the filter is considered efficient and capable of accurately estimating the state variables.

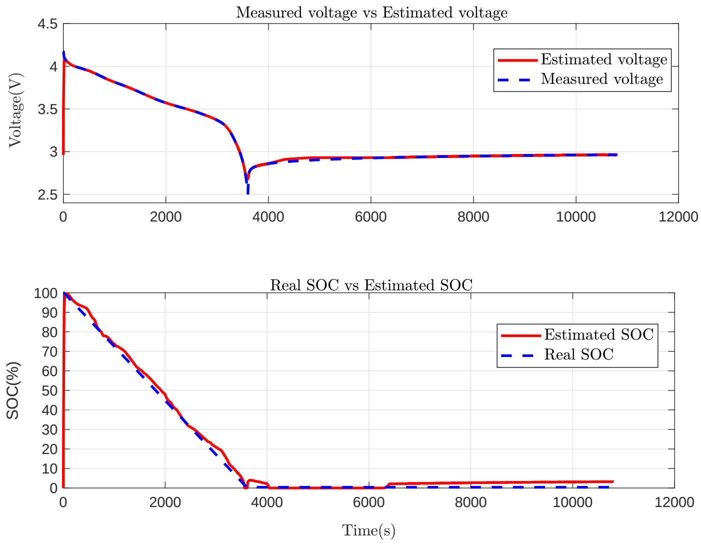

Figure 7: Validation results under Xilinx

5. Results of the real time implementation on FPGA

5.1. Real time validation using pre-recorded data

Prior to testing the developed observer on a real battery, an emulated test was conducted using pre-recorded current/voltage data from the battery. The results of this test, presented in Figure 8, indicate that the observer performs satisfactorily in real time. The current profile used corresponding to a battery discharge with a current step of 1C (2.5 A), and the SOC was initialized to 0%. The SOC reference was obtained using a coulomb meter initialized with the correct initial SOC and nominal capacity. A comparison of the results obtained from the emulated test and those from the simulation conducted under Xilinx, as shown in Figure 7, suggests that the observer performs similarly in both cases. Moreover, the implemented Kalman filter on FPGA was successful in minimizing the error between the measured voltage and the estimated voltage, enabling the estimated state of charge to converge to the exact value that cannot be measured.

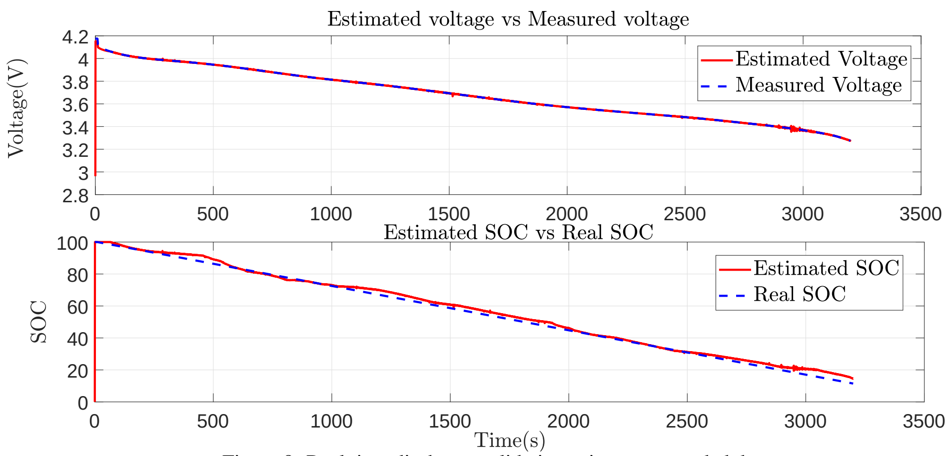

Figure 8: Real time discharge validation using pre-recorded data

5.2. Experimental validation of the observer

Having validated the observer in real time using pre-recorded data, the next step is to test it on the actual battery during discharge. To perform this experimental validation, we utilized the test bench shown in Figure 9. By subjecting the battery to a discharge cycle while running the observer, we can evaluate the accuracy of the observer's SOC estimates in a real-world scenario.

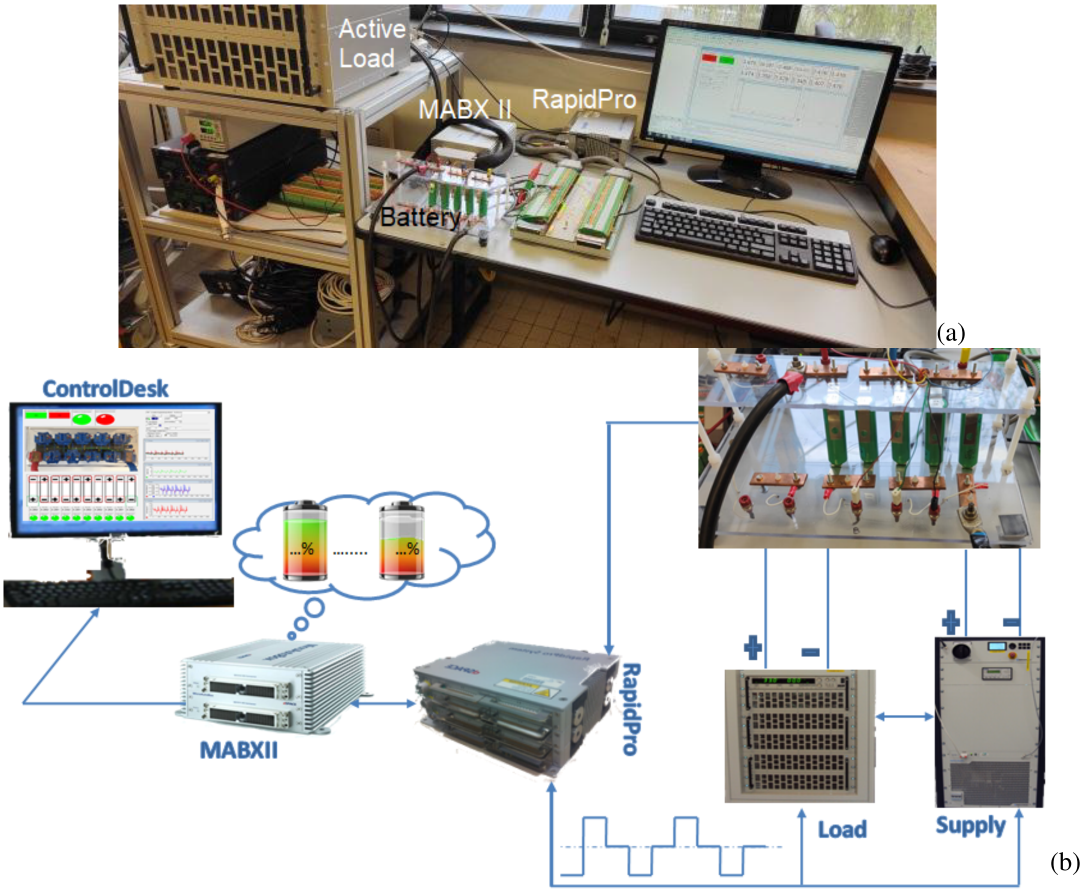

Figure 9: (a) Experimental test bench (b) Scheme of the platform

In order to perform experimental testing of the estimator, a cycle of current pulses (as shown in Figure 10) was generated and used as a set point for a programmable active load that was connected to the battery. The battery was then discharged using this active load.

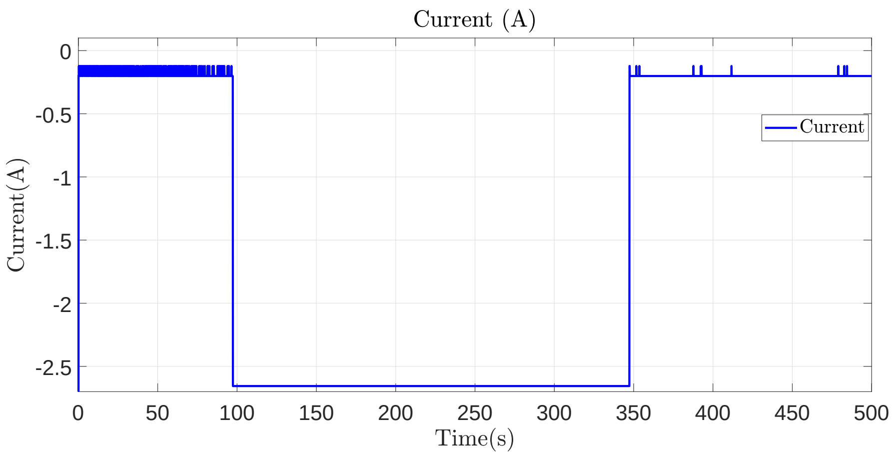

Figure 10: Discharge current pulses cycle

The experimental results for the first cell are presented in Figure 11. At the beginning of the current cycle The filter is able to correct the state of charge initialized at 0% . As the voltage decreases, the state of charge also decreases and the system can correct its state of charge automatically. However, a few oscillations occur during the estimation process, limiting the stabilization of the value. The oscillations are mainly due to the noise on the command and the measurement provided by the sensors. Therefore, a smoother filter is required to obtain values without oscillations.

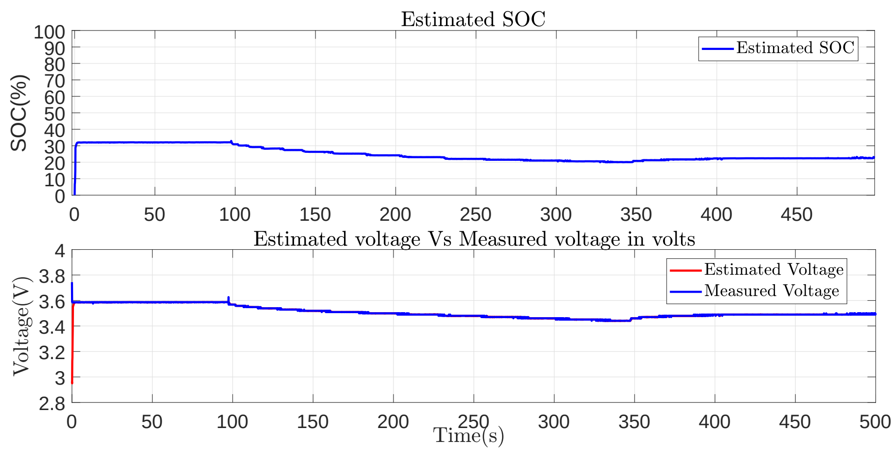

Figure 11: Experimental results for one cell in discharge

After presenting the estimation results for a single cell, and because the battery used in this study is made up of 5 cells connected in series, we must test the developed estimator on the entire battery pack. To test the developed estimator on the entire battery pack, the time division multiplexing technique illustrated in Figure 6 was added to the Kalman filter model. A current pulse cycle with a period of 3200 s and an amplitude of -2.5 A, similar to the one shown in Figure 10, was generated and used as a set point for a programmable active load H&H connected to the battery to discharge the cells. The obtained results for the whole battery pack are presented in Figure 12. The results demonstrate that the observer is able to estimate the voltage and SOC accurately not only for one cell but for the entire battery pack. The SOC and voltage of each cell can be determined based on the five curves obtained. The observer's ability to accurately estimate the voltage and SOC of each cell in the battery pack provides a significant advantage over previous studies that only estimated the voltage and SOC of the entire battery pack.

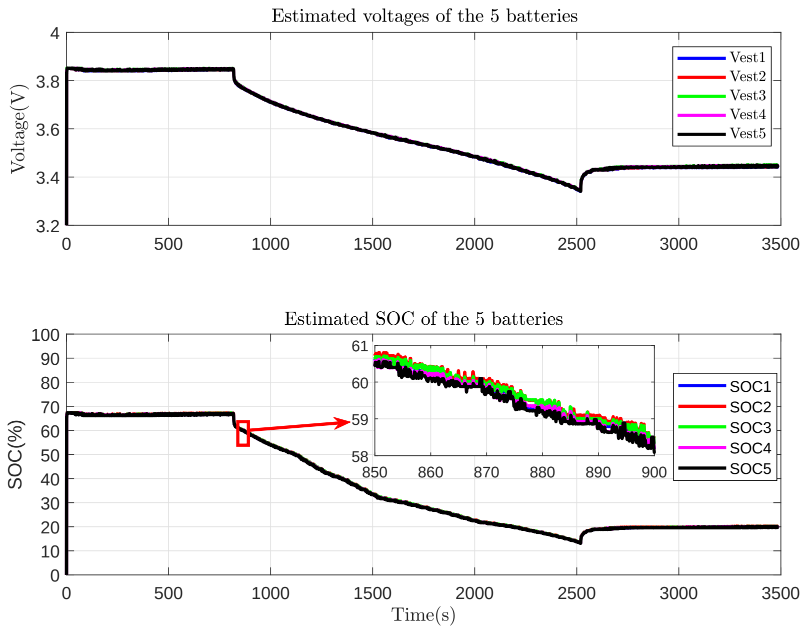

Figure 12: Experimental results for the entire battery pack in discharge

The execution time of the SOC observer has been evaluated to 2.5 µs. Given that a typical sample period for SOC observer is Te = 0.1 s, a Spartan 6 chip would have sufficient time to execute hundreds of SOC estimations during one sampling period, leaving enough time to observe other states such as internal temperature.

The implementation on the FPGA did not consume significant resources, as indicated by Figure 13 which shows the areas of resource usage.

Figure 13: Mapping of the areas of use of the resources.

Table 3 summarizes the synthesis results of the FPGA resources used. It can be noticed that despite the complexity of the program, we do not use all the resources available in our FPGA.

	Used	Available	Utilization
Slice Logic Utilization			
Number of Slice Registers (flip flops)	15395	184304	8%
Number of Slice LUTs	11442	92152	12%
Slice Logic Distribution			
Number of occupied Slices	4331	23038	18%
Number of MUXCYs	9148	46076	19%
I/O Utilization	180	498	36%
Number of DSP48A1s	94	180	52%

Table 3: Device Utilization Summary

6. Conclusion

Energy management in embedded applications is essential to optimize consumption and battery life. It requires accurate monitoring of the state of charge of batteries. This study has focused on the development of a state observer for estimating the voltage and state of charge of each cell in a lithium-Ion battery pack. The observer employs Kalman filter algorithm for Lithium-Ion batteries, which can correct the estimated state of charge even when initialized differently from the actual state of charge. The implementation of this complex algorithm on a low-cost Spartan 6 FPGA (< 20 euros) has been demonstrated to be highly efficient, enabling the observation of multiple batteries at once and reducing the cost of battery management systems. Experimental results demonstrate that the observer accurately estimates the voltage and state of charge of each cell, providing a significant advantage over previous studies that only estimated the voltage and state of charge of the entire battery pack. The low execution time and resource consumption of the observer make it a promising solution for real-time monitoring and control of lithium-Ion battery packs in various applications. While there were challenges in the implementation process due to noisy data, this can be addressed using appropriate filters to achieve accurate results. Overall, this study has provided a valuable contribution to the field of battery management systems and paves the way for further research in this area.

References

[1] G. J. May, A. Davidson, B. Monahov, Lead batteries for utility energy storage: A review, Journal of Energy Storage 15 (2018) 145–157. doi:https://doi.org/10.1016/j.est.2017.11.008.

[2] R. Morello, R. Di Rienzo, R. Roncella, R. Saletti, R. Schwarz, V. Lorentz, E. Hoedemaekers, B. Rosca, F. Baronti, Advances in li-ion battery management for electric vehicles, in: IECON 2018 - 44th Annual Conference of the IEEE Industrial Electronics Society, 2018, pp. 4949–4955. doi:10.1109/IECON.2018.8591185.

[3] A. A. Kebede, T. Coosemans, M. Messagie, T. Jemal, H. A. Behabtu, J. Van Mierlo, M. Berecibar, Techno-economic analysis of lithium-ion and lead-acid batteries in stationary energy storage application, Journal of Energy Storage 40 (2021) 102748. doi:https://doi.org/10.1016/j.est.2021.102748.

[4] S. Baljit, H.-Y. Chan, K. Sopian, Review of building integrated applications of photovoltaic and solar thermal systems, Journal of Cleaner Production 137 (2016) 677 – 689.

[5] A. Nasser-Eddine, B. Huard, J.-D. Gabano, T. Poinot, A two steps method for electrochemical impedance modeling using fractional order system in time and frequency domains, Control Engineering Practice 86 (2019) 96–104. doi:https://doi.org/10.1016/j.conengprac.2019.03.001.

[6] N. Collath, B. Tepe, S. Englberger, A. Jossen, H. Hesse, Aging aware operation of lithium-ion battery energy storage systems: A review, Journal of Energy Storage 55 (2022) 105634. doi:https://doi.org/10.1016/j.est.2022.105634.

[7] Z. Wang, G. Feng, X. Liu, F. Gu, A. Ball, A novel method of parameter identification and state of charge estimation for lithium-ion battery energy storage system, Journal of Energy Storage 49 (2022) 104124. doi:https://doi.org/10.1016/j.est.2022.104124.

[8] X. Liu, J. Yang, L. Wang, J. Wu, Bayesian information criterion based data-driven state of charge estimation for lithium-ion battery, Journal of Energy Storage 55 (2022) 105669. doi:https://doi.org/10.1016/j.est.2022.105669.

[9] M. Berecibar, I. Gandiaga, I. Villarreal, N. Omar, J. Van Mierlo, P. Van den Bossche, Critical review of state of health estimation methods of li-ion batteries for real applications, Renewable and Sustainable Energy Reviews 56 (2016) 572–587. doi:https://doi.org/10.1016/j.rser.2015.11.042.
[10] Y. Wang, J. Tian, Z. Sun, L. Wang, R. Xu, M. Li, Z. Chen, A comprehensive review of battery modeling and state estimation approaches for advanced battery management systems, Renewable and Sustainable Energy Reviews 131 (2020) 110015. doi:https://doi.org/10.1016/j.rser.2020.110015.
[11] A. Verani, G. Fieramosca, A. Colicelli, R. Di Rienzo, R. Saletti, R. Roncella, R. Schwarz, V. Lorentz, F. Baronti, Fpga accelerator for battery management systems in safety-critical applications, in: 2020 2nd IEEE International Conference on Industrial Electronics for Sustainable Energy Systems (IESES), Vol. 1, 2020, pp. 261–266. doi:10.1109/IESES45645.2020.9210671.
[12] M. Ul Hassan, S. Saha, M. E. Haque, S. Islam, A. Mahmud, N. Mendis, A comprehensive review of battery state of charge estimation techniques, Sustainable Energy Technologies and Assessments 54 (2022) 102801. doi:https://doi.org/10.1016/j.seta.2022.102801.
[13] N. Li, Y. Zhang, F. He, L. Zhu, X. Zhang, Y. Ma, S. Wang, Review of lithium-ion battery state of charge estimation, Global Energy Interconnection 4 (6) (2021) 619–630. doi:https://doi.org/10.1016/j.gloei.2022.01.003.
[14] Y. Guo, D. Yang, Y. Zhang, L. Wang, K. Wang, Online estimation of soh for lithium-ion battery based on ssa-elman neural network, Protection and Control of Modern Power Systems 7 (1) (2022) 40.
[15] D. Li, D. Yang, L. Li, L. Wang, K. Wang, Electrochemical impedance spectroscopy based on the state of health estimation for lithium-ion batteries, Energies 15 (18) (2022) 6665.
[16] G. Chen, Z. Liu, H. Su, Q. Zhang, Electrochemical model based state of charge estimation for lithium batteries with backstepping techniques, in: 2019 Chinese Control Conference (CCC), 2019, pp. 697–702. doi:10.23919/ChiCC.2019.8865913.
[17] A. K. Madsen, M. S. Trimboli, D. G. Perera, An optimized fpga-based hardware accelerator for physics-based ekf for battery cell management, in: 2020 IEEE International Symposium on Circuits and Systems (ISCAS), 2020, pp. 1–5. doi:10.1109/ISCAS45731.2020.9181073.
[18] X. Tian, B. Jeppesen, T. Ikushima, F. Baronti, R. Morello, Accelerating state-of-charge estimation in fpga-based battery management systems, in: 6th Hybrid and Electric Vehicles Conference (HEVC 2016), 2016, pp. 1–6. doi:10.1049/cp.2016.0964.
[19] J. Wu, C. Jiao, M. Chen, J. Chen, Z. Zhang, SOC estimation of li-ion battery by adaptive dual kalman filter under typical working conditions, in: 2019 IEEE 3rd International Electrical and Energy Conference (CIEEC), IEEE, 2019. doi:10.1109/cieec47146.2019.cieec-2019558.
[20] J. Yan, G. Xu, Y. Xu, B. Xie, Battery state-of-charge estimation based on h filter for hybrid electric vehicle, in: 2008 10th International Conference on Control, Automation, Robotics and Vision, IEEE, 2008. doi:10.1109/icarcv.2008.4795563.
[21] R. Morello, F. Baronti, X. Tian, T. Chau, R. D. Rienzo, R. Roncella, B. Jeppesen, W. H. Lin, T. Ikushima, R. Saletti, Hardware-in-the-loop simulation of FPGA-based state estimators for electric vehicle batteries, in: 2016 IEEE 25th International Symposium on Industrial Electronics (ISIE), IEEE, 2016. doi:10.1109/isie.2016.7744903.
[22] F. Baronti, W. Zamboni, N. Femia, H. Rahimi-Eichi, R. Roncella, S. Rosi, R. Saletti, M.-Y. Chow, Parameter identification of li-po batteries in electric vehicles: A comparative study, in: 2013 IEEE International Symposium on Industrial Electronics, IEEE, 2013. doi:10.1109/isie.2013.6563887.
[23] N. Otero, H. Rahimi-Eichi, J. J. Rodriguez-Andina, M.-Y. Chow, FPGA implementation of an observer for state of charge estimation in lithium-polymer batteries, in: 2014 International Conference on Mechatronics and Control (ICMC), IEEE, 2014. doi:10.1109/icmc.2014.7231839.
[24] Y. Song, W. Liu, H. Li, Y. Zhou, Z. Huang, F. Jiang, Robust and accurate state-of-charge estimation for lithium-ion batteries using generalized extended state observer, in: 2017 IEEE International Conference on Systems, Man, and Cybernetics (SMC), IEEE, 2017. doi:10.1109/smc.2017.8122937.
[25] Y. Feng, J. Du, C. Xue, F. Han, X. Yu, Estimation of SoC of batteries using terminal sliding-mode observer, in: 2018 IEEE 8th Annual International Conference on CYBER Technology in Automation, Control, and Intelligent Systems (CYBER), IEEE, 2018. doi:10.1109/cyber.2018.8688224.
[26] K. Abhinav, S. Mija, Observer based sliding mode control for 3 DOF helicopter system, in: 2021 International Conference on Intelligent Technologies (CONIT), IEEE, 2021. doi:10.1109/conit51480.2021.9498495.
[27] B. Kumar, N. Khare, P. K. Chaturvedi, Advanced battery management system using MATLAB/simulink, in: 2015 IEEE International Telecommunications Energy Conference (INTELEC), IEEE, 2015. doi:10.1109/intlec.2015.7572447.
[28] B. Kumar, N. Khare, P. Chaturvedi, Fpga-based design of advanced bms implementing soc/soh estimators, Microelectronics Reliability 84 (2018) 66–74. doi:https://doi.org/10.1016/j.microrel.2018.03.015.
[29] C. Unterrieder, R. Priewasser, S. Marsili, M. Huemer, Battery state estimation using mixed kalman/hinfinity, adaptive luenberger and sliding mode observer, in: 2013 IEEE Vehicle Power and Propulsion Conference (VPPC), IEEE, 2013. doi:10.1109/vppc.2013.6671667.
[30] D. Jiani, W. Youyi, W. Changyun, Li-ion battery SOC estimation using particle filter based on an equivalent circuit model, in: 2013 10th IEEE International Conference on Control and Automation (ICCA), IEEE, 2013. doi:10.1109/icca.2013.6565047.
[31] X. Shen, W. Zhu, Y. Yang, J. Xie, L. Huang, A state of charge estimation method based on APSO-PF for lithium-ion battery, in: 2021 IEEE 4th International Electrical and Energy Conference (CIEEC), IEEE, 2021. doi:10.1109/cieec50170.2021.9510942.
[32] R. Restaino, W. Zamboni, Comparing particle filter and extended kalman filter for battery state-of-charge estimation, in: IECON 2012 - 38th Annual Conference on IEEE Industrial Electronics Society, IEEE, 2012. doi:10.1109/iecon.2012.6389247.
[33] C. Pulavarthi, R. Kalpana, P. Parthiban, State of charge estimation in lithium-ion battery using model based method in conjunction with extended and unscented kalman filter, in: 2020 International Conference on Power Electronics and Renewable Energy Applications (PEREA), IEEE, 2020. doi:10.1109/perea51218.2020.9339816.
[34] P. Shi, Y. Zhao, Application of unscented kalman filter in the SOC estimation of li-ion battery for autonomous mobile robot, in: 2006 IEEE International Conference on Information Acquisition, IEEE, 2006. doi:10.1109/icia.2006.305934.
[35] Z. Cui, L. Kang, L. Li, L. Wang, K. Wang, A combined state-of-charge estimation method for lithium-ion battery using an improved BGRU network and UKF, Energy 259 (2022) 124933. doi:10.1016/j.energy.2022.124933.
[36] A. Laurin, V. Heiries, M. Montaru, State-of-charge and state-of-health online estimation of li-ion battery for the more electrical aircraft

based on semi-empirical ageing model and sigma-point kalman filtering, in: 2021 Smart Systems Integration (SSI), IEEE, 2021. doi:10.1109/ssi52265.2021.9466997.

[37] G. Plett, Extended kalman filtering for battery management systems of lipb-based hev battery packs: Part 3. state and parameter estimation, Journal of Power Sources 134 (2) (2004) 277–292. doi:https://doi.org/10.1016/j.jpowsour.2004.02.033.

[38] V. Pop, H. J. Bergveld, D. Danilov, P. P. Regtien, P. H. Notten, Battery management systems: Accurate state-of-charge indication for battery-powered applications, Vol. 9, Springer Science & Business Media, 2008.

[39] M. Wu, L. Qin, G. Wu, State of charge estimation of power lithium-ion battery based on an affine iterative adaptive extended kalman filter, Journal of Energy Storage 51 (2022) 104472. doi:https://doi.org/10.1016/j.est.2022.104472.

[40] R. R. Richardson, D. A. Howey, Sensorless battery internal temperature estimation using a kalman filter with impedance measurement, IEEE Transactions on Sustainable Energy 6 (4) (2015) 1190–1199. doi:10.1109/TSTE.2015.2420375.

[41] F. Baronti, R. Roncella, R. Saletti, W. Zamboni, Fpga implementation of the mix algorithm for state-of-charge estimation of lithium-ion batteries, in: IECON 2014 - 40th Annual Conference of the IEEE Industrial Electronics Society, 2014, pp. 5641–5646. doi:10.1109/IECON.2014.7049364.

[42] R. Zhou, Y. Liu, E. Brodeur, Z. Li, J. Guo, A reverse-boot enabled embedded computing system on soc-fpga for prognostics and health management: An application on li-ion batteries, in: 2019 IEEE 9th Annual Computing and Communication Workshop and Conference (CCWC), 2019, pp. 0800–0805. doi:10.1109/CCWC.2019.8666519.

[43] N. NOURA, K. COS, L. BOULON, S. JEMEI, Online identification of battery internal resistance under extreme temperatures, in: 2020 IEEE Vehicle Power and Propulsion Conference (VPPC), IEEE, 2020. doi:10.1109/vppc49601.2020.9330928.

[44] D. Babu, A. Kumar, J. Roychowdhury, FPGA based model predictive controller for dynamic power management of a battery powered electric car, in: 2012 12th International Conference on Intelligent Systems Design and Applications (ISDA), IEEE, 2012. doi:10.1109/isda.2012.6416565.

[45] Y. Song, D. Liu, Y. Peng, FPGA-based implementation of lithium-ion battery SOH estimator using particle filter, in: 2020 IEEE International Instrumentation and Measurement Technology Conference (I2MTC), IEEE, 2020. doi:10.1109/i2mtc43012.2020.9128439.

[46] S. Buller, M. Thele, R. De Doncker, E. Karden, Impedance-based simulation models of supercapacitors and li-ion batteries for power electronic applications, IEEE Transactions on Industry Applications 41 (3) (2005) 742–747. doi:10.1109/TIA.2005.847280.

[47] D. V. Do, C. Forgez, K. El Kadri Benkara, G. Friedrich, Impedance observer for a li-ion battery using kalman filter, IEEE Transactions on Vehicular Technology 58 (8) (2009) 3930–3937. doi:10.1109/TVT.2009.2028572.

[48] D. Pritsker, Hybrid implementation of extended kalman filter on an fpga, in: 2015 IEEE Radar Conference (RadarCon), 2015, pp. 0077–0082. doi:10.1109/RADAR.2015.7130974.

[49] L. Gagneur, C. Forgez, A. L. D. Franco, On-line adaptive tuning of a lithium-ion battery cell state of charge observer, in: 2013 IEEE Energy Conversion Congress and Exposition, 2013, pp. 307–314. doi:10.1109/ECCE.2013.6646716.

[50] M. Elkholy, H. Metwally, M. Farahat, T. Senjyu, M. Elsayed Lotfy, Smart centralized energy management system for autonomous microgrid using fpga, Applied Energy 317 (2022) 119164. doi:https://doi.org/10.1016/j.apenergy.2022.119164.

[51] E. Monmasson, L. Idkhajine, M. N. Cirstea, I. Bahri, A. Tisan, M. W. Naouar, Fpgas in industrial control applications, IEEE Transactions on Industrial Informatics 7 (2) (2011) 224–243. doi:10.1109/TII.2011.2123908.

[52] J. J. Rodriguez-Andina, M. D. Valdes-Pena, M. J. Moure, Advanced features and industrial applications of FPGAs—a review, IEEE Transactions on Industrial Informatics 11 (4) (2015) 853–864. doi:10.1109/tii.2015.2431223.

[53] F. Vendrame, H. Rabbab, N. Damay, C. Forgez, Influence of aging on sei and charge transfer resistances and their dependence on current and temperature for a li-ion nca+nmc/graphite cell, in: 14th international conference Electrimacs, 2022.

[54] F. Vendrame, C. Forgez, M. Sayegh, Reduced model for fast simulation of a lithium-ion battery pack taking into account current and state of charge dispersion, in: 2022 IEEE Energy Conversion Congress and Exposition (ECCE), 2022, pp. 1–6. doi:10.1109/ECCE50734.2022.9948095.